RARE EARTH COBALT PERMANENT MAGNET MATERIALS FOR ELECTROMECHANICAL ENERGY CONVERSION DEVICES

G. Lafrate, et al

Army Electronics Command
Fort Monmouth, New Jersey

1972

177

IAFRATE, ROSS, ROTHWARF
and CAMPAGNOULO

RARE EARTH COBALT PERMANENT MAGNET MATERIALS FOR ELECTROMECHANICAL ENERGY CONVERSION DEVICES

G. Iafrate, R. L. Ross, F. Rothwarf, C. Campagnoulo†
USA Electronics Technology and Devices Laboratory (ECOM)
Fort Monmouth, New Jersey 07703

† Harry Diamond Laboratories, Washington, D.C.

I. INTRODUCTION

In the past few years, considerable research (1-13) has been conducted on binary and ternary alloy systems of the 3d transition elements with metals of the rare-earth group (elements with nuclear charge 21, 39 and 57 through 71). These studies have revealed many new ferro- and ferrimagnetic substances. The most impressive of these new alloys are those based on the hexagonal intermetallic cobalt rare-earth (RE) compounds Co_5RE. Strnat (1) has reported on the interesting magnetic properties of such compounds as Co_5Y, Co_5Ce, Co_5Pr and Co_5Sm. The particular alloys Co_5Sm and $Co_5Sm_{0.5}Pr_{0.5}$ represent a major breakthrough in the development of permanent magnet materials in that they possess extraordinarily high maximum energy products and extremely large intrinsic coercive fields. The advent of these remarkable materials calls for imaginative new approaches to the design of both static and dynamic permanent magnet devices. In this paper, we present new designs which utilize these materials in the development of a compact electronically tunable high field dc magnet for use in microwave filters and power limiters as well as in the design of power generators for use in artillery fuzing applications.

Section II is a discussion of permanent magnet materials. The concepts of maximum energy product and intrinsic coercivity are considered. A comparison of the Co_5RE alloys with commercially popular permanent magnet materials is also presented.

In Section III, the specific design relationships for the Co_5RE magnet materials are given. Particular use is made of the fact that these materials have, to a good approximation, a linear demagnetization characteristic and also possess low recoil permeabilities.

Begin→145

In Section IV, detailed analyses of the tunable permanent magnet and the power generator are given. Results based on feasibility models, built at our laboratories, are presented and discussed. A promising fuze power system resulting from using a power generator in conjunction with the fluidic oscillator developed at Harry Diamond Laboratories is presented.

In Section V, we summarize our results.

II. SUMMARY OF PERMANENT MAGNET MATERIALS

The alloys, Co_5Ce and Co_5Sm, possess unusual permanent magnet qualities. In general, such qualities are manifested by the demagnetization characteristic (the second quadrant of the B-H hysteresis curve) of the material. The usefulness of a particular material in permanent magnet applications is determined principally by the remanent induction, B_r, which measures the intrinsic magnetization remaining in the material when the applied field is removed and the coercive field, H_c, which determines the field necessary to reduce the induction to zero. An important criterion in considering the utility of a permanent magnet material in design applications is the so-called maximum energy product, $(B\cdot H)_{max}$. If one takes the product of B and H for all points along the demagnetization curve and plots this product versus B, a maximum occurs at the point, say, (B', H'). For materials whose demagnetization curve is not linear, such as the curve for Alnico in Fig. 1, B' and H' can readily be found by solving for the point of intersection of a straight line, passing through the point (B_r, H_c) and the origin, with the demagnetization curve. For materials with linear demagnetization curves such as that of Co_5RE in Fig. 1, it is easily shown that $B' \cong B_r/2$ and $H' \cong H_c/2$ so that $(B\cdot H)_{max} \cong B_rH_c/4$. The maximum energy product, $(B\cdot H)_{max}$, is a measure of the magnetic field energy stored per unit volume of material. The new Co_5Sm and $Co_5Pr_{0.5}Sm_{0.5}$ magnets have been produced with $(B\cdot H)_{max}$ values as high as 23 and 26 mega-Gauss-Oersted (MGOe), respectively. By comparison, the various commonly used Alnicos have a $(B\cdot H)_{max}$ value of about 3-5 MGOe.

Traditionally, $(B\cdot H)_{max}$ has been thought of as the main criteria for excellence in permanent magnet materials. This follows from the fact that the amount of material necessary to produce a given volume is inversely proportional to $(B\cdot H)_{max}$. However, its usefulness, as a criteria is limited to static cases. In dynamic applications one is concerned with the coercivities H_c and H_{ci} of a material. H_c has already been defined as the field which reduces the induction B to zero in the second quadrant. H_{ci} is the field at which the magnetization, M (commonly referred to as the intrinsic induction B_i), defined by the relation $B = H+4\pi M(H) = H+B_i$, goes to zero. It is the difference $(H_{ci}-H_c)$ which determines the usefulness of a material for dynamic applications. For materials such as the

Alnicos, H_{ci} is approximately equal to H_c. Furthermore, these values are usually small, ranging from 0.5 to 1.5 kOe. Thus, such materials are easily demagnetized by transient fields. In contrast, the Co_5RE magnets $H_{ci} \gg H_c$. For Co_5Sm, specially heat-treated samples have been produced with $H_{ci} \cong 18$ kOe and $H_c \cong 9$ kOe. This means that the B-H curve remains linear into the third quadrant of the hysteresis loop (Fig. 2) for a negative field up to 18 kOe and will recoil nearly to the B_r value of 9.7 kOe, with almost no loss of flux, when H is again reduced to zero. Table I gives a comparison of certain important parameters for several commonly used magnet materials.

III. MAGNETIC CIRCUIT DESIGN

In designing magnetic circuits for the most efficient use of the new magnet materials, one tries to choose a load-line such that it intersects the demagnetization curve at an optimal operating point, namely at a point where the stored magnetic energy is a maximum. The load-line is a straight line through the origin of the B-H plane and is given by

$$B/H = -k \tag{1}$$

where k depends on the geometry of the magnetic circuit. For a ring type circuit with a small gap-length, l_g, $k = l_m A_g / l_g A_m$ where l_m, A_m are the length and cross-sectional area, respectively, of the magnetic material and A_g is the cross-sectional area of the gap.

In our applications, the load-line equations are derived by making use of the well-known magnetic circuit analog (14) of Ohm's law

$$\Phi(\text{flux}) = F(\text{magnetomotive force})/R(\text{reluctance}) \tag{2}$$

and the flux conservation theorem (14)

$$\oint d\Phi = 0 \tag{3}$$

where $d\Phi$ is given by $d\Phi = \vec{B} \cdot \vec{ds}$.

The first stage in the development of design calculations requires the specification of the demagnetization curve for the chosen magnet material. For the Co_5RE materials, the demagnetization curves are essentially linear (see Section II) and can be approximated by the straight-line equation

$$B = \mu_m H + B_r \tag{4}$$

where μ_m, the recoil permeability of the magnet material in the demagnetization region, is given by the ratio, B_r/H_c. The simultaneous set of solutions to Eqs. (1,4) are easily obtained as

$$B_m = \frac{kB_r}{(k+\mu_m)} \quad , \quad H_m = -\frac{B_r}{(k+\mu_m)} \quad . \tag{5}$$

The B_m and H_m values are clearly a function of k and represent the operating point for the magnet.

The second stage in design calculations requires the determination of the load-line (or k). Having specified a magnet material of length l_m and cross-sectional area A_m, it is necessary to calculate the operating point required to deliver a field B_g to an air gap with reluctance $R_g = l_g/A_g(\mu_a = 1)$, l_g being the length and A_g being the cross section area of the gap. This calculation would be rather routine if the magnet reluctance, $R_g = l_m/\mu_m A_m$, were negligibly small (μ_m very large). But, in point of fact, the permeabilities of the Co_5RE materials are typically of the order of unity, thereby making the reluctances of these magnets comparatively large. Thus, the Co_5RE materials behave as magnetomotive sources with high internal reluctance. For these materials, one is concerned with a "terminal" magnetomotive force, T. For a magnet material with reluctance R_m and an "open" circuit magnetomotive force $F = -H_m l_m$, the analogous "terminal" magnetomotive force is given by

$$T = - H_m l_m \left(\frac{R_c}{R_m + R_g} \right) \quad . \tag{6}$$

Using this notion, Eqs. (2,3) can be written as

$$T = R_g \Phi_g \tag{7}$$

and

$$B_m A_m - B_g A_g = 0 \tag{8}$$

where T is given in Eq. (6). By successively multiplying and dividing Eqs. (7,8), while using the fact that $B_g = H_g$, we obtain

$$\frac{B_m}{H_m} = - \frac{l_m}{A_m} \left(\frac{1}{R_m + R_g} \right) \equiv k \tag{9}$$

and

$$- B_m H_m V_m \left(\frac{R_g}{R_m + R_g} \right) = B_g^2 V_g \tag{10}$$

where V_m and V_g are the respective volumes of the magnet and air-gap. Eq. (9) represents the desired load-line equation whereas Eq. (10) is a manifestation of conservation of magnetic energy. Since k is now established for this particular problem (see Eq. 9), the operating point for the magnet can be obtained from Eq. (5) as

$$B_m = B_r \frac{R_m}{(R_g + 2R_m)} \tag{11}$$

and

$$H_m = - H_c \frac{(R_m + R_g)}{(R_g + 2R_m)} \quad . \tag{12}$$

In order to transfer the maximum available magnetic energy from the magnet material to the gap, we utilize the analog criterion for maximum energy transfer in electrical circuits, namely, that the reluctances of the magnet and gap be equal, thus yielding

$$l_m/A_m = \mu_m R_g \quad . \tag{13}$$

This condition restricts the operating point given in Eqs. (11,12) to

$$B_m = B_r/3 \tag{14}$$

and

$$H_m = 2H_c/3 \quad . \tag{15}$$

Putting these expressions into the energy relation of Eq. (10), we obtain

$$(B_r H_c) V_m/9 = B_g^2 V_g \quad . \tag{16}$$

An explicit expression for V_m is then found to be

$$V_m = (9B_g^2 V_g/B_r H_c) \equiv l_m A_m \tag{17}$$

From Eqs. (13,17), unique expressions for l_m and A_m can be obtained as

$$l_m = 3B_g l_g/H_c \tag{18}$$

and

$$A_m = 3B_g A_g/B_r \quad . \tag{19}$$

Eqs. (18,19) represent the design criteria relating the field in the gap to the geometry of the circuit. However, in the foregoing discussion, it was tacitly assumed that flux leakage effects were negligible. In practice, such effects are significant and are handled in a variety of ways depending on the particular geometry of the magnet circuit. Nevertheless, in the applications section that follows, the above design criteria are utilized, to within a limited degree of accuracy, with both gap and magnet parameters serving as independent variables.

Lastly, it is interesting to note that the points, B_m and H_m, found in Eqs. (14,15), do <u>not</u> correspond to B' and H', the values corresponding to $(B \cdot H)_{max}$. This follows directly as a consequence of assigning a non-zero reluctance to the magnet. If the magnet reluctance was negligibly small so that $R_m \sim 0$ when compared to R_g, then the desired operating point would be found, by Eqs. (4,9), to be $B_m = B_r/2 \equiv B'$ and $H_m = H_c/2 \equiv H'$, in coincidence with $(B \cdot H)_{max}$.

IAFRATE, ROSS, ROTHWARF
and CAMPAGNOULO

IV. APPLICATIONS

A. Electronically Controlled Magnets for Tunable Microwave Filters

1. Introduction

An existing in-house ECOM program (15) is concerned with the development of magnetically tunable bandpass filters covering the frequency ranges from 18 to 26.5 GHz (K-band), and from 26.5 to 40 GHz (Ka-band). These filters are to be utilized as fast-tuning front-end preselectors in microwave receivers designed for these frequencies. They make use of the principle of ferromagnetic resonance to achieve very sharp bandpass characteristics. A sharp resonance occurs at the angular frequency ω given by $\omega = \gamma H$ where γ is the gyromagnetic ratio and H is the applied magnetic field. Preliminary design models incorporate low-loss single-crystal yttrium iron garnet (YIG) spheres as the filter resonator material, chiefly because of its low linewidth and high Curie temperature. YIG has a γ of 2.59 GHz/kOe. Although it has a narrow linewidth and therefore a low loss, YIG requires moderately high magnetic fields to resonate in the K- and Ka- bands. These range from 6 kOe at 18 GHz to 14 kOe at 40 GHz. Such high external magnetic field requirements have led to the development of electromagnet structures of relatively large size, weight, and power consumption. In addition, the YIG spheres must be temperature stabilized, usually at 85° C. The large electromagnet structure then acts as an adverse thermal mass which must be maintained at some elevated temperature necessitating further power consumption in addition to that normally required to maintain a given field or to electronically sweep a band.

There have been attempts to develop alternate materials, e.g., hexagonal ferrites of the M, Y, W, and U types, for use as filter resonators which would require less applied magnetic field for resonance than conventional YIG. However, to date, such attempts have remained relatively unsuccessful due to the unacceptable linewidths of these materials. The obvious alternative is to replace the electromagnet structures with one utilizing Co_5RE materials. An example of the previously used electromagnet structure is shown in Fig. 3. Each coil of this structure consists of approximately 3000 turns of No. 19 AWG wire necessitating a total power consumption of nearly 40 watts to produce the requisite 9 kOe field at 26 GHz. The corresponding size reduction through use of the Co_5RE material is evidenced in Fig. 4, wherein 150 turns of No. 22 AWG consuming less than 0.5 watts result in producing the same 9kOe field as the electromagnet above. Whereas the electromagnet requires a static current to maintain a constant field-bias operating point about which the current is then varied to tune the filter, the same operating point can be established without any power dissipation in the Co_5RE structure by mechanically adjusting the gap with the knurled screws shown in Fig. 4. A current through the coil about one arm of the structure serves to vary the field around the operating point. This technique represents a significant departure from, and a resultant

advantage over, the previous mode of microwave filter operation. Using the Co_5RE model shown in Fig. 4 fields up to 20 kG (the saturation field for soft steel) are realizable which in turn, would make possible filters in the 40 to 60 GHz range.

2. Mathematic Analysis

Here, we utilize some of the concepts presented in Sec. III in the actual construction and analysis of the model dc magnet structure shown in Fig. 4. This structure includes two rings of Co_5Ce type C magnet material furnished by the Sel-Rex Corporation, Nutley, N.J. They were axially magnetized and set on one steel plate of the magnetic circuit with their magnetic moments parallel. The disk dimensions were 3.18 cm.OD, 1.59 cm.ID, and 0.8 cm. in length. The magnetic circuit was then completed by sliding the other plate in position and adjusting the screws to supply the desired field in the gaps. The widths and lengths of the plate bodies were slightly greater than one and two magnet diameters, respectively. The plate bodies were rounded at each end with nearly the same radius of curvature as the magnets.

From the electrical analogy, the magnetic circuit associated with such a magnet design may be thought of as a parallel combination of two identical magnetomotive sources, possessing two internal reluctances, R_m, in series with a load reluctance, R_L. The load reluctance is considered to be a parallel combination of gap reluctance, R_g representing the space between the screw faces, and the "loss" reluctance, R_ℓ representing the space between the arms of the magnetic circuit, associated with one major source of flux loss to the gap. Thus, the terminal magnetomotive force for this circuit may be written as

$$T = - H_m l_m \left[R_L/(\tfrac{1}{2}R_m + R_L)\right] \tag{20}$$

where

$$R_L = R_g R_\ell/(R_g + R_\ell) \quad . \tag{21}$$

The term $R_m/2$ in the denominator of Eq. (20) indicates that the effective magnet area exposed to the gap increases twofold. Therefore, when two magnets are positioned in parallel combination, the amount of flux available for delivery to the gap, doubles. Thus, for this particular magnet design, the flux conservation theorem of Eq. (3) may be written as

$$B_m\, 2A_m - \phi_g - \phi_\ell = 0 \quad . \tag{22}$$

In addition, the "Ohm's Law" expression, equivalent to Eq. (7), is

$$-H_m l_m \left[R_L/(\tfrac{1}{2}R_m + R_L)\right] = R_L(\phi_g + \phi_\ell), \tag{23}$$

In dividing Eqs. (22,23), we obtain one load-line equation

$$B_m/H_m = l_m/2A_mR_L \equiv k \quad . \tag{24}$$

Putting the above value of k into Eq. (5), we obtain the operating point of the magnet, B_m and H_m, as

$$B_m = R_mB_r/(R_m + 2R_L) \tag{25}$$

and

$$H_m = - 2R_LH_c/(R_m + 2R_L). \tag{26}$$

Thus, the terminal magnetomotive force in Eq. (20) can be re-expressed as

$$T = H_c l_m[2R_L/(R_m + 2R_L)] \quad . \tag{27}$$

Since the flux concentrated at R_g or R_ℓ is given by $\phi_i = T/R_i$, ($R_i = R_g$ or R_ℓ), it then follows that the magnetic fields associated with the respective reluctances are $B_i = \phi_i/A_i$, A_i being the appropriate geometrical area. The explicit expressions for the magnetic fields in these regions are:

$$B_i = H_c(l_m/l_i)\,[2R_L/R_m + 2R_L)], \; i = g \text{ or } \ell \quad . \tag{28}$$

3. Results

For the particular dimensions of the magnet in Fig. 4 the theoretical values of fields obtained using Eq. (28) are B_g=16.5 kG and B_ℓ =0.81 kG. The actual fields measured using a Hall probe Gaussmeter were B_g = 14.5 kG and B_ℓ = 0.72 kG, thus indicating an error of about 12% in the theoretical predictions. Errors of this magnitude are not uncommon (16) when flux leakage effects are ignored. Thus, one can say that the fields calculated, while ignoring flux leakage effects, provide an upper bound to the experimental fields expected in the respective gaps.

A dc current through the coil wrapped around one of the arms of the magnet structure shown in Fig. 4, serves as an additional means of biasing the magnetic field in the gap between the screw faces. With a gap of 0.08cm, for zero dc current, a gap field B_g = 11.5 kG was obtained in the test magnet structure. B_g could be varied through the fields defining the Ka-band limits, i.e., 9.1-14.0 kG by changing the current in to coil from -1.10 amps. to +1.10 amps. Since the coil has a resistance of 0.60 ohms, the power needed to sweep to the band limits in either direction was only 0.73 watts. It should be noted that our model has a much smaller gap and volume than would be needed for the necessary Ka-or K-band microwave cavities and a somewhat larger power would be needed to sweep an actual full scale model, having a gap-length of 0.353 cm and a volume of 0.875 cm^3. The calculated power under this set of operative dimensions is 1.05 watts.

185

It is also interesting to note that the volume of Co_5Ce material needed to supply a sufficiently large bias field to a gap for a suitable Ka- or K-Band waveguide assembly is calculated from Eq. (17) to be about 30 cm^3, i.e., nearly 2 in^3 or two of the cubes shown in Fig. 3. This represents a significant reduction in size and weight from the existing magnet coils. Moreover, the equivalent calcuation, utilizing Co_5Sm (with approximately the same mass density as Co_5Ce), shows that a volume of about 8 cm^3 in magnet material would be necessary to accomplish the same objectives. This latter result is quite impressive.

B. Moving Coil Generator for Use in a Fluidic Power Source

1. Introduction

For some time the Harry Diamond Laboratories have been developing a variety of devices that convert pneumatic energy into a significant amount of electrical energy for use in fuzing systems. These devices, called fluidic generators, involve a new fuzing principle in that each device represents a combination of a new power source with a new safing and arming signature. These innovations provide improved safety and reliability, especially for systems with no spin and only small setback forces such as mortar shells and rockets.

The generator, when used as a power supply in a projectile or missile, obtains its driving energy from ram-air through an opening in the nose of the shell. A schematic drawing of one such device is shown in Fig. 5. The air, after passing through an annular nozzle, generates acoustic energy via an oscillating jet impinging on a resonating cavity. The acoustic energy drives a metal diaphragm at resonance. In the version shown in Fig. 5, a reed attached to the diaphragm is driven to modulate magnetic flux in a coil. This generates an emf in the coil. The output voltage is then rectified or amplified before utilization in a fuzing function. The flux modulation generator used in all previous versions of this device have some inherent limitations due to the permeability vs field characteristics of the modulator materials available, which restrict the amount of electrical power which one can extract from the pneumatic (ram-air) power available. The rare-earth cobalt materials offer the possibility of designing more efficient magnetic circuits for such devices because of the higher flux density B that can be achieved in the gap of a magnetic circuit by using these new materials.

2. Description of Moving Coil Generator

One of the devices we have studied makes use of a circular coil moving in the annular gap of a magnetic circuit having cylindrical symmetry. The schematic cross-section drawing of the

moving coil generator being considered is shown in Fig. 6A. A radial magnetic field is established in the gap G formed by the flux concentrating projections on the soft steel central post and the inner edge of the soft steel washer.

The moving coil is not spirally wound concentric with the post axis. Rather, it is formed from a flat rectangular loop of N turns. This loop is then closed on itself, so that its shorter sides are vertical, to form a circle whose average radius is that of the gap as shown in Fig. 6B. The coil is then glued to a vertical support that is attached to the center of the vibrating diaphragm. This coil support also has a fine nylon centering pin which fits into a guide hole in the steel center post. The rod attaching the coil support to the diaphragm is threaded so that the position of the coil in the gap can be adjusted. The magnetic circuit is designed to furnish a given field in the gap, B_g, by using the analysis presented in Section III above.

3. Mathematical Analysis

The voltage induced in the coil will be

$$\mathcal{E} = 10^{-8} N \frac{d\phi}{dt} \text{ , volts.} \tag{29}$$

The flux $\phi(t)$ intercepted by the coil at any given time will be

$$\phi(t) = B_g \Delta A(t) \tag{30}$$

where B_g is the magnetic induction in the gap and $\Delta A(t)$ is that portion of the coil area instantaneously in the gap. $\Delta A(t)$ is explicitly given as $\Delta A(t) = 2\pi \bar{R}_g Y(t)$, where $\bar{R}_g$ is the average gap radius as well as the coil radius, r_c. $Y(t)$ is that portion of the coil height instantaneously in the gap. The coil should be so positioned that its area does not completely intercept that of the gap, i.e., a given vibration should cause the coil to intercept more or less flux. $Y(t)$ is given by $Y(t) = Y_0 + a \sin \omega t$ where ω is the angular frequency with which the coil is driven, and a is the amplitude of the driving oscillation. At time $t = 0$, Y_0 is the height of the coil in the gap. Thus, the voltage induced in the coil is

$$\mathcal{E} = 2\pi \times 10^{-8} N \bar{R}_g a\omega \cos \omega t \equiv \mathcal{E}_{pk} \cos \omega t \text{ .} \tag{31}$$

The average power delivered to a load R_L, equal to the resistance of the coil R_c, is given by

$$\bar{P} = \bar{\mathcal{E}}^2/2R_c \equiv \mathcal{E}_{pk}^2/4R_c \text{ .} \tag{32}$$

If the coil height is small compared to its length, the resistance of the coil can be approximated assuming that the coil length is given by $4\pi N\bar{R}_g$ so that $R_c = 4\pi N\bar{R}_g r_w$ where r_w is the resistance per unit length for the wire used to wind the coil. The average power delivered becomes

$$\bar{P} = \frac{\pi \times 10^{-16} N \bar{R}_g A^2 B_g^2 \omega^2}{4 r_w} \text{ , watts.} \qquad (33)$$

Here we have assumed the load to be real rather than complex. The calculation is readily done for a complex load.

4. Results

The power to be obtained is given by Eq. (33). A preliminary model to test this prediction has been built and is shown in Fig. 6. The coil used in our generator model consists of 100 turns of (28.8 ft) of #44 gauge copper wire ($r_w = 8.2 \times 10^{-2}$ Ω/cm). The gap dimensions were determined by considering the gap volume needed to sustain 10 kG. Utilizing Eqs. (20,21), with l_m = .8 cm and $A_m = 6.0$ cm^2 for Co_5Ce, we obtain l_g = .13 cm. A_g is given by

$$A_g = 2\pi \bar{R}_g Y_g = \left(\frac{B_r}{3B_g}\right) A_m \ . \qquad (34)$$

Choosing a value of $\bar{R}_g$ = .65 cm, we obtain of value of Y_g = .28 cm by direct use of Eq. (34).

In practice, a field of about 5kG was obtained due to large flux leakage. Preliminary tests at low driving amplitudes have verified Eq. (33). However, detailed tests of the generator when coupled to the fluidic oscillator remain to be done.

Assuming that the fluidic generator (17) can drive the diaphragm into oscillation with a = 0.01 cm and f = 2.5×10^3 Hz, the power resulting from use of Eq. (33) is predicted to be about 0.13 watts, a power sufficient to drive many electronic fuze systems (18). This output can be increased considerably by changing the parameters chosen, e.g., B_g can be doubled or tripled easily by using Co_5Sm material and amplitude and frequency can be increased by suitable diaphragm and oscillator design so that factors of twenty or more may well be possible in the power.

V. SUMMARY AND CONCLUSIONS

The great potential for military device applications inherent in the new rare-earth cobalt permanent magnet materials has been pointed out. Important magnetic circuit design criteria peculiar to these materials have been developed and two specific devices have been given as examples as to how these principles are employed. The electronically tunable magnet for microwave filters and power limiters that now can be built with these materials will lead to a significant reduction in size, weight, and power consumption when compared to those previously developed. The moving coil generator also offers

promise of increased power for electronic fuzes. However, suitable interfacing of this generator with the fluidic oscillator remains to be finalized.

Overall, these new magnet materials offer a great potential for improving a variety of military devices dictated by the requirements of the modern electronic battlefield.

REFERENCES

1. K. L. Strnat, Cobalt No. 36, 133 (1967).
2. K. H. J. Buschow, Z. Metallkunde, 57, 728 (1966).
3. K. H. J. Buschow, J. Less Comm. Metals 11, 204 (1966).
4. R. Lemaire, Cobalt Nos. 32 and 33 (Sept. and Dec. 1966) 132 and 201.
5. V. I. Chechernikov et al., Fiz. Metal. metalloved 20, 299 (1965).
6. A.E. Ray, Acta Cryst. 21, 426 (1966).
7. W. Ostertag and K. Strnat, Acta Cryst. 21, 560 (1966).
8. K. L. Strnat, G. Hoffer, J. Olson, W. Ostertag, and J.J. Becker, J. Appl. Phys. 38, 1001 (1967).
9. K.A. Gschneider, Jr., "Rare Earth Alloys," D. Van Nostrand Co., Princeton (1961).
10. K.K. Das, Design News, 14 April 1969.
11. E. A. Nesbit, R.H. Willens, R.C. Sherwood, E. Buehler, and J.H. Wernick, Appl. Phys. Letters 12, 361 (1968).
12. J.J. Becker, F.E. Luborsky, and D. Luther Martin, IEEE Transactions on Magnetics, MAG-4, 239 (1968).
13. J.J. Becker, IEEE Transactions on Magnetics, MAG-4, 239 (1968).
14. R.J. Parker and R.J. Studders, Permanent Magnets and Their Application, John Wiley and Sons, Inc., 1962.
15. R.L. Fjerstad and D.B. Weller, Fort Monmouth Research and Development Technical Report ECOM-0528-P004-M1303, October 1969.
16. S. Chikazumi, Physics of Magnetism, John Wiley & Sons, Inc., New York.
17. C.J. Campagnoulo and R.N. Gottron, Proceedings of the 24th Power Sources Symposium, p. 42 (1970).
18. Proposal for Improving Beehive Fuzing (Confidential), Picatinny Arsenal, May 1970.

189

IAFRATE, ROSS, ROTHWARF
and CAMPAGNOULO

TABLE I

Material	B_r kG	H_c kOe	H_{ci} kOe	$(B \cdot H)_{max}$ MGOe	Density gram/cm^3	Cost $ per/lb
Co_5 Ce	5.6	4.8	6.2	6.7	8.3	8
Co_5 Sm	9.5	9.0	18.0	23.0	5.6	35
Co Pt	6.2	4.3	5.3	9.0	15.5	2,000
Alnico VIII	8.0	1.6	1.6	5.0	7.3	30
Strontium Ferrite	3.2	3.0	4.0	2.4	5.1	4

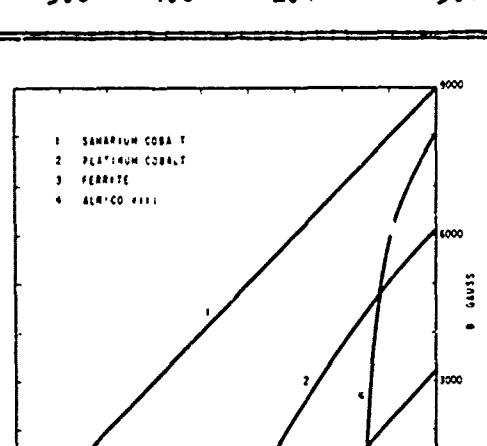

Fig. 1. Demagnetization curve for various permanent magnet materials.

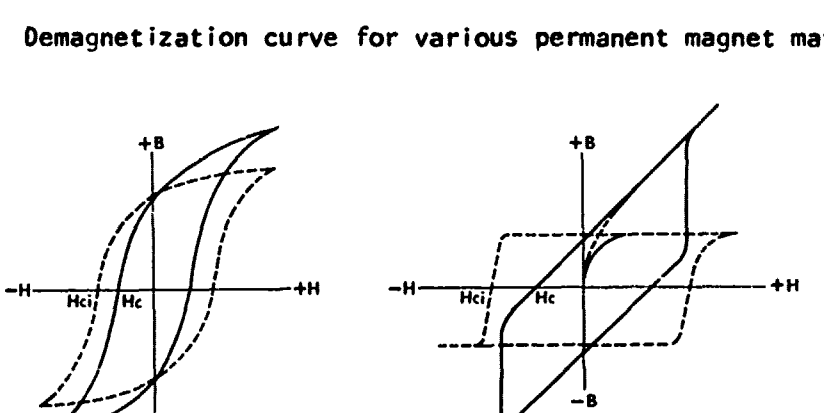

Fig. 2. Comparison of magnetization, M, and induction, B, as a function applied field, H.

Fig. 3. Photograph of present magnet used in filter designs.

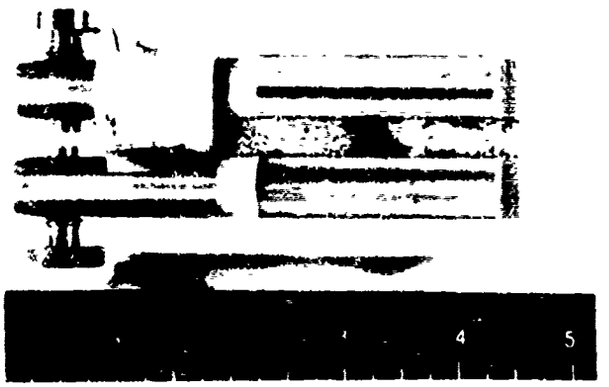

Fig. 4. Photograph of prototype tunable dc magnet.

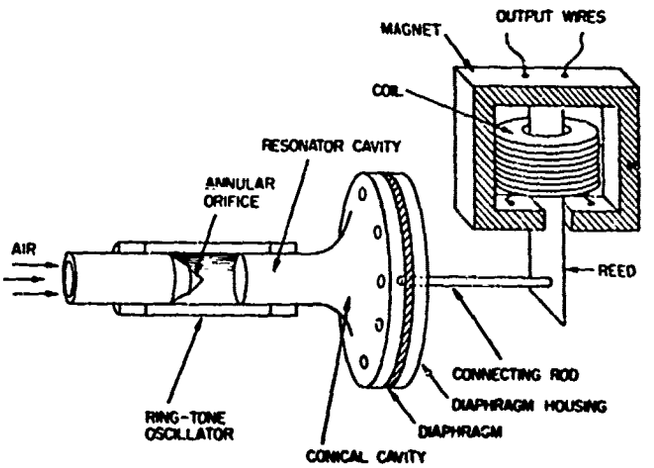

Fig. 5. Schematic of fluidic generator with ringtone oscillator.

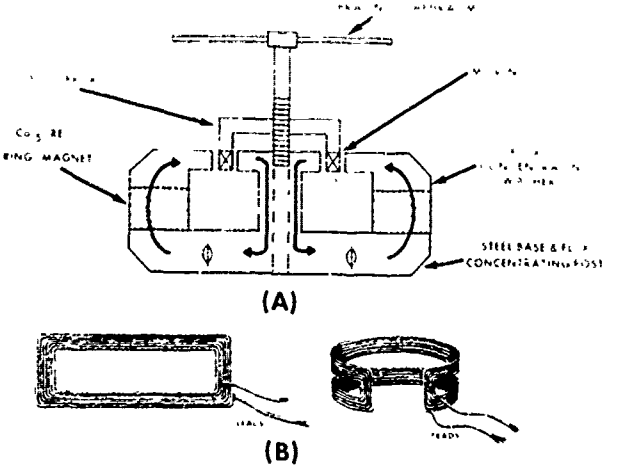

Fig. 6,I. Schematic of moving coil assembly.

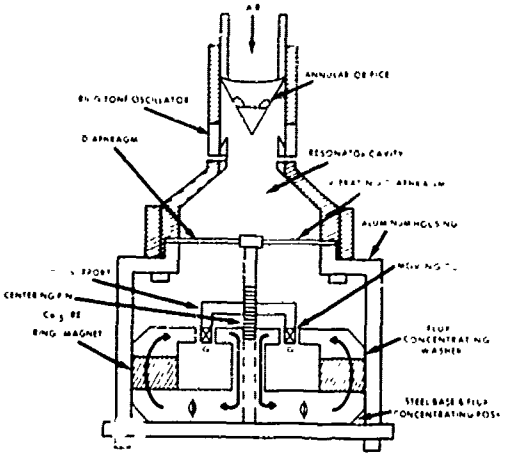

Fig. 6,II. Schematic of ac generator.

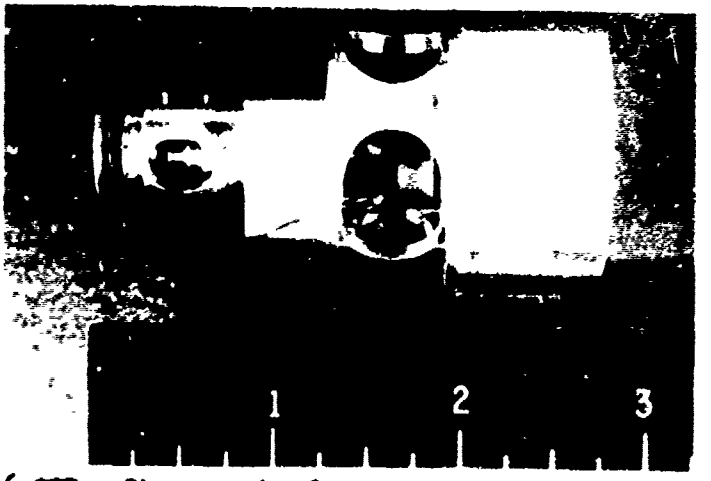

Fig. 6,III. Photograph of prototype ac generator.